Detecting Hydrogen Bonding by NMR Relaxation of the Acceptor Nuclei**

Alessandro Bagno,*[a] Sébastien Gerard,[b] Jan Kevelam,[c] Enzo Menna,[a] and Gianfranco Scorrano[a]

Abstract: The formation of hydrogen bonds (HB) between phenol or *N*-methyltrifluoroacetamide and several acceptors (pyridine, carbonyl compounds, nitriles, amides) in CCl_4 or $CHCl_3$ been investigated through the analysis of NMR relaxation times (T_1) of the heteronuclei (^{14}N and ^{17}O) directly involved in the HB interaction. Thus, a comparison is made between such T_1 values (corrected for changes in molecular dynamics and motional anisotropy) and electric field gradients calculated by ab initio methods for the acceptor molecules, both isolated and in 1:1 or 2:1 hydrogen-bonded complexes. When other effects are properly accounted for, there is a good agreement between theoretical and experimental electric field gradient (efg) changes. The noticeable difference found between CCl_4 or $CHCl_3$ as solvents is discussed in relation to the presence of phenol oligomers, and the non-negligible HB donor power of $CHCl_3$.

Keywords: ab initio calculations · hydrogen bonding · NMR spectroscopy · quadrupolar relaxation · solvation

Introduction

Among weak interactions,[1] the hydrogen bond (HB) is the strongest, and is in fact a key process in nature.[2] A typical HB is shown in Scheme 1, where A (HB donor) is an electronegative atom or group bearing an acidic hydrogen, and B (HB acceptor) is an atom with basic properties.

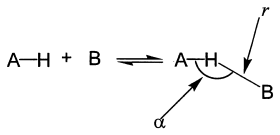

Scheme 1. A typical hydrogen bond: **A** (electronegative) is hydrogen bond donor) is an electronegative atom or group bearing an acidic hydrogen, and **B** is hydrogen acceptor.

Hydrogen bonding determines the properties of many condensed-phase systems (including water), and is arguably the strongest force governing solvent effects on reactivity. Hence, accounting for HB interactions is required for understanding chemical reactivity in polar solvents.

The energy of a HB between neutral molecules is 3–5 kcal mol^{-1}; HBs involving ionic species are stronger (ca. 10 kcal mol^{-1}), the upper limit being given by HF_2^- (40 kcal mol^{-1}).[3] The HB complex possesses a preferred geometry[4–6] (Scheme 1), defined by the HB distance (r, generally around 2 Å) and the angle formed by the A–H bond and the acceptor atom (α, usually close to 180°). With certain donor/acceptor pairs, the barrier for proton exchange may be very low or absent. Such "low-barrier" HBs are believed to be involved in enzymatic catalysis, and their properties are being intensely investigated.[7]

Owing to its fundamental and practical interest, HB is studied by a wide variety of techniques. Hence, we will just indicate some methods that have a bearing on the present work, and list a few recent developments with no pretence of completeness.

Fundamental investigations of HB have been carried out by, for example IR spectroscopy,[8–12, 13a] calorimetry,[13] and ^{19}F NMR spectroscopy.[13b, 13d] However, when several alternative HB sites are present, very few experimental methods provide evidence for individual hydrogen bonds and identify the atoms involved. The existence of a HB, and its structural parameters, are inferred from the spatial proximity of potential donor and acceptor moieties, as revealed by X-ray crystallography in the solid state or, in solution, by NMR spectroscopy through techniques based on dipolar couplings (NOEs) between protons, or ^{13}C and ^{15}N. Solute–solvent interactions in general have also been investigated with such techniques.[14, 15] Since these experiments exploit dipolar relaxation, they cannot involve the observation of quadrupolar nuclei (such as ^{14}N or ^{17}O) which are, in most cases, the

[a] Dr. A. Bagno, Dr. E. Menna, Prof. G. Scorrano
Centro CNR Meccanismi Reazioni Organiche
Dipartimento di Chimica Organica, Università di Padova
via Marzolo 1, 35131 Padova (Italy)
Fax: (+39) 0498275239
E-mail: alex@chor.unipd.it

[b] Dr. S. Gerard
Visiting student from the University of Versailles (France) under the Erasmus program

[c] Dr. J. Kevelam
Visiting student from the University of Groningen (The Netherlands) under the Erasmus program

[**] Supporting information for this contribution is available on the WWW under http://www.wiley-vch.de/home/chemistry/

  0947-6539/00/0616-2915 $ 17.50+.50/0

acceptors involved. Therefore, the actual acceptor site is often indirectly estimated from other internuclear distances.

Other NMR studies are based on the variation of the exchange rate with the solvent[16] and isotope effects.[17] More recent works have reported on the detection of HB through a) inter-residue $^{13}C-^{15}N$ scalar coupling (transmitted through the HB) in RNA,[18, 19] peptides[20] and low-barrier HBs;[7f] b) ^{1}H chemical shift anisotropy;[21] c) ^{2}H nuclear quadrupolar coupling constants;[22] d) studies at very low temperatures on systems in slow exchange conditions[23] (all methods requiring isotopically enriched materials). NMR dipolar couplings, directly measured in the solid state, have also been recently employed to this effect,[24] which may provide an alternative to X-ray crystallography if solid-state HBs are investigated.

The formation of a hydrogen bond has also been studied by means of quantum chemical calculations[1, 2, 6] at the Hartree–Fock[25] or correlated[26] levels. In this context, we also mention "non-conventional" HBs involving, for example negatively charged hydrogens or π systems as acceptors, C–H groups as donors, anti-HBs, etc. Since these often elusive but important interactions are difficult to study experimentally,[27] a great effort is being devoted to their theoretical investigation.[28]

Theoretical methods can, in principle, completely characterize the energy and structure of the HB complex, and predict its spectroscopic properties. Generally, such calculations are carried out on simplified model systems, but the solvent effect on HB has been recently modeled by reaction field methods.[29]

One of the most interesting problems in this respect is related to the preferential HB formation on a specific acceptor, when more than one site is available in the same molecule. This condition is always met in biomolecules, such as proteins and DNA, and is the basis for their complex secondary structures, and ultimately for molecular recognition and enzyme catalysis.

From these considerations stems the interest for any method of investigation of HB formation based on the direct observation of the acceptor atom. In order to develop an approach of this kind, one should find a probe for HB formation which should be experimentally observable and undergo theoretically predictable changes upon formation of the HB. In this work, we have used changes in the electric field gradient at the acceptor nuclei to this effect. We will show how this parameter can be observed and predicted, and how the information it provides is related to HB formation.

Method

NMR measurements: The longitudinal relaxation of quadrupolar nuclei ($I > ½$; e.g. ^{14}N, ^{17}O) is almost entirely due to the quadrupolar mechanism, which derives from the interaction between the nuclear quadrupole moment Q and the electric field gradient (efg) at the nucleus.[30] The latter is originated by any asymmetry in the local charge distribution. The efg (dE/dr) decreases as $1/r^3$, and therefore in covalent species it is largely intramolecular in origin. In the extreme narrowing limit the longitudinal relaxation rate is given by Equation (1):

$$\frac{1}{T_1} = \frac{3\pi^2}{10}\frac{2I+3}{I^2(2I-1)}\chi^2\left(1+\frac{\varepsilon^2}{3}\right)\tau_c \qquad (1)$$

where $\chi = eQq_{zz}/h$ is the nuclear quadrupolar coupling constant, q_{zz} is the largest principal component of $\mathbf{q}$, $\varepsilon = |q_{xx} - q_{yy}|/q_{zz}$ its asymmetry parameter[31] and τ_c the rotational correlation time.

Since the T_1 in solution depends on both q_{zz} and ε, which cannot be separated, it is convenient to define an effective coupling constant, $\chi_{eff} = \chi^2(1+\varepsilon^2/3)$ with which calculated efg values can be compared (see below). Then Equation (1) can be recast as $1/T_1 = K\chi_{eff}\tau_c$, showing that T_1 depends both on the molecular structure (χ_{eff}) and dynamics (τ_c). Upon HB formation, the symmetry (and therefore the efg) at the acceptor nucleus obviously changes, which may result in a T_1 variation, normally reflected also in the line width $W_{1/2}$.[30] Previous studies carried out in our laboratory have demonstrated that the NMR relaxation of quadrupolar nuclei can pinpoint the most stable ionic form deriving from an acid–base reaction on a compound bearing more than one available ionization site, because proton transfer to or from nitrogen or oxygen generally causes a large efg change which can be modeled by quantum chemical calculations and is experimentally detected as substantial changes in T_1 of the relevant nuclei.[32]

Proton transfer and HB are qualitatively similar, and in fact the latter can be viewed as the preliminary stage for the former, however with a longer B–H equilibrium distance and no charge separation. Then one can legitimately expect that HB formation entails the same qualitative changes found for proton transfer, albeit reduced in magnitude (owing to the $1/r^3$ distance dependence of the efg). This expectation, however, calls for a careful evaluation of all factors involved in quadrupolar relaxation, like changes in molecular dynamics.

This dependence in Equation (1) is given by τ_c, which is related to the viscosity of the solution, the temperature and the hydrodynamic volume of the species.[30] Hence, upon formation of the HB complex τ_c is expected to change, as the motion of the complex may be slower than that of the free acceptor. Since we carried out our experiments at constant temperature, and we found a viscosity increase by only ca. 10% upon addition of the donor, remaining changes in τ_c are due to changes in the hydrodynamic volume, which cannot be accurately determined. This problem can be avoided determining directly the change in τ_c, by determining changes in the dipolar relaxation rate ($1/T_1^{DD}$) of a suitable ^{13}C nucleus in the acceptor molecule, since $1/T_1^{DD} \propto \tau_c/r_{CH}^6$, where r_{CH} is the distance between the carbon of interest and a close proton. The DD contribution to T_1 is obtained by the NOE factor η, since $T_1^{DD} = T_1\eta_{max}/\eta$, where $\eta_{max} = \gamma_H/2\gamma_C$.[30] Given the decrease of the DD relaxation rate with $1/r_{CH}^6$, it is convenient to observe a carbon atom directly bonded to a hydrogen, in order to have larger NOE values and shorter T_1 relaxation times. Moreover, absence of independent mobility of the C–H bond with respect to the acceptor group is required. On the other hand, from a theoretical viewpoint the orientation of the C–H vector should be the same as of q_{zz} for it to have the same

  0947-6539/00/0616-2916 $ 17.50+.50/0 Chem. Eur. J. 2000, 6, No. 16

correlation time; this becomes important only if the motion is highly anisotropic (see below). Once the dynamics contribution to the T_1 change is known, we can isolate the term depending on the electric field gradient (χ_{eff}), as follows.

According to Equation (1), the efg change is $\chi_{eff}^{HB}/\chi_{eff}^{0} = (T_1^{0}/T_1^{HB})(\tau_c^{0}/\tau_c^{HB})$, where the free and H-bonded acceptor are indicated with a "0" or "HB" superscript, respectively. The change in τ_c, that is τ_c^{0}/τ_c^{HB}, can be obtained by means of ^{13}C NMR measurements as mentioned above, assuming that r_{CH} is not affected by the HB (which is reasonable, considering the relatively weak interaction occurring at a remote site), so that $\tau_c^{0}/\tau_c^{HB} = T_1^{DD,HB}/T_1^{DD,0}$. The incomplete formation of HB is accounted for observing that all NMR spectra showed signals for one species only, which implies that B and AHB are under fast exchange conditions. Hence, the observed relaxation rate in the presence of the donor is the average of individual rates, weighted by the amount of free or H-bonded acceptor. Combining these relations (see Experimental Section for details) we obtain Equation (2), yielding the experimental efg variation, which can be compared with that predicted theoretically.

$$\chi_{eff}^{R} = \frac{\chi_{eff}^{HB}}{\chi_{eff}^{0}} = \frac{1 + \frac{1}{x_{HB}}\left(\frac{T_1^{0}}{T_1} - 1\right)}{1 + \frac{1}{x_{HB}}\left(\frac{T_1^{DD,0}}{T_1^{DD}} - 1\right)} \qquad (2)$$

Quantum chemical calculations: We calculated the efg values at the HF/6-311G(d,p) level using geometries optimized at the same level for donors, acceptors, and HB complexes. We also tested the performance of lower-level calculations, optimizing the geometry of HB complexes (many of which are quite large in size) at the HF/6-31G(d,p) level, that is running HF/6-311G(d,p)//6-31G(d,p) calculations. Some test calculations were also run at the DFT B3LYP/6-311G(d,p)//B3LYP/6-31G(d,p) level.[33]

The Cartesian components of the efg tensor **q** are easily calculated from the ground-state wave function.[34] Nevertheless, this property does not converge smoothly upon improving the method or the basis set size.[35] Diagonalization of **q** yields the three principal components (q_{xx}, q_{yy}, q_{zz}) as the eigenvalues, and their orientation (Euler angles with respect to the molecular coordinate system) as the eigenvectors, from which χ_{eff} can be evaluated [see Eq. (1)]. All calculations were run with Gaussian 98.[36]

Results

ab initio Calculations: The minimal 1:1 donor:acceptor structure was calculated in most cases, except some carbonyl acceptors. In fact, since the carbonyl oxygen has two lone pairs, such acceptors can accept hydrogens from two different donors, as investigated theoretically[37] and by X-ray crystallography.[38] Hence, we also ran some calculations for 2:1 complexes of carbonyl acceptors.

Calculated efg values are reported in terms of q_{zz}, ε, and χ_{eff}; for HB complexes the change $\chi_{eff}^{R} = \chi_{eff}^{HB}/\chi_{eff}^{0}$ is also given. This quantity will be compared with the corresponding experimental values obtained from Equation (2). CF_3OH was initially employed as a model HB donor, but was eventually replaced by the molecules experimentally studied, namely phenol and *N*-methyltrifluoroacetamide (MTA), since it became apparent that efg changes induced by each donor were markedly different.

The full data set, containing individual components of **q** at all theoretical levels employed, as well as the data for CF_3OH systems, is provided as Supporting Information. The results (energies, HB geometrical parameters, absolute and relative χ_{eff} values) for HB complexes of PhOH and MTA at the highest level of calculation are summarized in Table 1.

Extent of formation of the HB complex: The reversible formation of an HB complex is characterized by an equilibrium constant K_{HB}, from which x_{HB} can be extracted. Several quantitative HB acidity and basicity scales, built from calorimetric or IR data, are known.[8–11] Such scales were constructed using solutions far less concentrated than those required for this study. Furthermore, the required data for some compounds we have studied, for example MTA, are not available. Hence, we determined x_{HB} directly by means of FT-IR measurements.[10, 11] Values of x_{HB} obtained with the two methods sometimes differ substantially. For the processing of NMR data we used experimental FT-IR x_{HB} values where available, and Taft's in remaining cases. However, the results (in terms of χ_{eff}^{R}) were found not to depend much on the assumed x_{HB}, within a range of reasonable values.

Choice of model systems: Some simple organic molecules belonging to different acceptor functionalities (pyridine, cyano, carbonyl, and amide) were selected, the acceptor nuclei being nitrogen and oxygen. We initially used phenol as the donor, since many experimental studies have been done on its HB complexes. Given the extraordinary biological relevance of hydrogen bonds between amides, we also employed *N*-methyltrifluoroacetamide ($CF_3CONHCH_3$, MTA) as a model donor. Its HB properties are not reported, but a very low HB acceptor power can be inferred from the low pK_{HB} value of $CF_3CON(CH_3)_2$.[13d] FT-IR measurements indicated that MTA is a weaker donor than phenol.

Carbon tetrachloride has been widely adopted as HB-inert solvent[8–11] and was initially used as solvent, but it is a poor solvent for MTA and its complexes, which were studied in chloroform. Since the two solvents ($CHCl_3$ is a weak but not negligible donor[8]) were found to differ far more than expected, some phenol complexes were also studied in $CHCl_3$ for comparison.

NMR measurements: Although the line width of signals of quadrupolar nuclei is generally a good approximation to T_1, since $W_{1/2}$ ($= 1/\pi T_2^*$) and $T_1 \approx T_2^*$, the direct measurement of T_1 is preferable, since line widths are more liable to errors. Hence, for the more sensitive ^{14}N nucleus we determined T_1 values. The ^{17}O nucleus presents experimental difficulties due to its very low natural abundance (0.037%).[30] Therefore, unless the signal was relatively narrow or when we used ^{17}O-enriched material, we assumed $T_1 = T_2^*$.

Table 1. Structural parameters, energy, and electric field gradients from ab initio calculations for donors, acceptors and HB complexes.[a]

Acceptor/Donor	E_b[b]	r[c]	α[d]	Nucleus	χ_{eff}[e]	χ_{eff}^R[f]
free donors						
PhOH				^{17}O	158.3	
MTA[g]				^{14}N	25.7	
pyridine				^{14}N	37.4	
[h]				^{14}N	32.3	
PhOH	−7.6	2.015	168.4	^{14}N	29.9	0.80
PhOH[h]	−9.8	2.015	168.3	^{14}N	24.8	0.77
PhOH dimer	−10.0	1.707; 1.953	166.9; 166.0	^{14}N	27.9	0.75
MTA	−7.2	2.115	170.5	^{14}N	30.2	0.81
acetonitrile				^{14}N	27.4	
PhOH	−5.8	2.150	174.0	^{14}N	23.1	0.84
MTA	−6.2	2.251	157.0	^{14}N	23.5	0.86
benzonitrile				^{14}N	27.6	
PhOH	−5.8	2.151	174.5	^{14}N	23.0	0.84
MTA	−6.2	2.249	158.5	^{14}N	23.4	0.85
formaldehyde				^{17}O	218.4	
2 $CHCl_3$	−7.3	2.314; 2.314	160.0; 160.0	^{17}O	185.5	0.85
2 CCl_4[i]	1.3	3.537; 3.613 [j]		^{17}O	218.2	1.00
Acetone				^{17}O	181.2	
PhOH	−7.6	1.971	166.1	^{17}O	157.7	0.87
2 PhOH	−13.5	2.006; 2.035	167.0; 160.1	^{17}O	139.7	0.77
MTA	−6.6	2.053	179.1	^{17}O	168.7	0.93
benzaldehyde				^{17}O	171.9	
[h]				^{17}O	152.3	
PhOH	−7.0	1.987	141.8	^{17}O	152.5	0.89
PhOH[h]	−10.8	1.848	170.1	^{17}O	135.8	0.89
2 PhOH	−17.0	2.012; 2.069	170.5; 149.0	^{17}O	133.1	0.77
MTA	−11.8	2.049	174.7	^{17}O	147.9	0.86
2 MTA	−17.1	2.133; 2.124	163.4; 171.9	^{17}O	136.5	0.79
***N*,*N*-dimethylformamide**				^{17}O	136.0	
				^{14}N	27.5	
PhOH (O)	−8.8	1.919	169.0	^{17}O	95.2	0.70
				^{14}N	23.6	0.86
PhOH (N)	−3.2	2.339	154.2	^{17}O	109.0	0.80
				^{14}N	24.2	0.88
2 PhOH (O)	−15.8	1.945; 1.996	171.0; 152.4	^{17}O	85.4	0.63
				^{14}N	21.0	0.76
MTA (O)	−9.2	1.973	174.2	^{17}O	90.1	0.66
				^{14}N	24.1	0.88
2 MTA (O)	−15.9	2.036; 2.068	171.9; 162.6	^{17}O	89.9	0.66
				^{14}N	21.0	0.76
***N*,*N*-dimethylbenzamide**				^{17}O	117.7	
				^{14}N	30.2	
PhOH (O)	−8.8	1.913	172.8	^{17}O	104.0	0.88
				^{14}N	26.6	0.88
PhOH (N)	−4.1	2.198	161.0	^{17}O	125.4	1.07
				^{14}N	26.8	0.89
2 PhOH (O)	−15.5	1.929; 2.003	161.0; 171.6	^{17}O	106.1	0.90
				^{14}N	23.2	0.77
MTA (O)	−8.8	1.958	171.4	^{17}O	107.9	0.92
				^{14}N	26.3	0.87
2 MTA (O)	−16.6	2.008; 2.001	172.1; 170.0	^{17}O	99.3	0.84
				^{14}N	23.6	0.78

[a] Selected data; see the Supporting Information for the full data set. Electric field gradients and geometries calculated at the HF/6–311G(d,p) level, except where otherwise indicated. For amide acceptors, the accepting nucleus is given in brackets. [b] Binding energy (kcal mol^{-1}): $E_b = E_{complex} - (E_{donor} + E_{acceptor})$, not corrected for the basis set superposition error. [c] HB distance [Å] (Scheme 1). [d] HB angle [degrees] (Scheme 1). [e] Effective nuclear quadrupole coupling constant in MHz^2 (1 MHz^2 = 10^{12} s^{-2}) for the given nucleus (^{17}O, ^{14}N) in the acceptor molecule. The following values for the nuclear quadrupole moments Q were used: ^{14}N, 2.02; ^{17}O, −2.558 fm^2.[48] [f] efg change with respect to the acceptor: $\chi_{eff}^R = \chi_{eff}^{HB}/\chi_{eff}^0$. [g] $CF_3CONHCH_3$. Calculations involving MTA were carried out with the conformer having the *N*-methyl group *cis* to the oxygen atom, which is more stable than the *trans* one (by 7 kcal mol^{-1}); induced efg changes are very similar. [h] B3LYP/6–311G(d,p)//B3LYP/6–31G(d,p). [i] HF/6–311G(d,p)//3–21G. [j] Distance between *C*Cl_4 and *CO*.

Concentration and solvent effects on the NMR parameters of pyridine and phenol: Decreasing the concentration of pyridine in CCl_4 from 1.0 to 0.05 M causes a small deshielding of ^{14}N ($\Delta\delta = 4$) and T_1 increase (from 1.59 to 1.64 ms). The latter change provides no evidence of any peculiar phenomenon other than changes in viscosity. We also determined ^{13}C T_1 and NOE values for phenol and pyridine solutions, both separately and in mixture (0.5 M in CCl_4 and $CHCl_3$) (Table 2).

Table 2. ^{13}C-NMR data for phenol and pyridine (0.5 M in CCl_4 and $CHCl_3$).

Solvent	assignment	δ	T_1 [s]	η	T_1^{DD} [s]
phenol					
CCl_4	C-1	155.3	32.8	0.9	75.0
	C-2	115.6	4.4	1.6	5.3
	C-3	129.8	4.5	1.4	6.3
	C-4	121.1	3.1	1.8	3.4
$CHCl_3$[a]	C-1	155.3	44	0.6	148 (89)
	C-2	115.3	8.9	1.7	6.3 (6.3)
	C-3	129.7	8.9	1.6	10.8 (6.5)
	C-4	120.9	7.3	1.7	8.5 (5.1)
phenol (+py)					
CCl_4	C-1	157.6	23.4	1.0	49.0
	C-2	115.9	3.3	1.9	3.5
	C-3	129.5	3.2	1.9	3.4
	C-4	119.6	2.0	2.0	2.0
pyridine					
CCl_4[e]	C-2	150.2	17.0	1.1	30.7
	C-3	123.6	17.5	1.1	31.6
	C-4	135.5	18.6	1.2	30.8
$CHCl_3$	C-2	149.6	14.5	1.6	18.0
	C-3	123.6	14.5	1.5	19.1
	C-4	135.9	12.8	1.5	17.0

[a] T_1^{DD} values in brackets are corrected for the lower viscosity of $CHCl_3$ as T_1^{DD} (corr.) = T_1^{DD} [$\eta(CHCl_3)/\eta(CCl_4)$]. η ($CHCl_3$) = 0.58 cP, η (CCl_4) = 0.97 cP at 20 °C,[48] and it is assumed that their ratio is equal to that of our solutions at 25 °C.

Even though the mobility of phenol and pyridine should be similar (judging from their similar size), the T_1^{DD} values of phenol are smaller than those of the corresponding carbon atoms in pyridine, which suggests some degree of association for phenol under these conditions. In order to improve our understanding of the solvent effect on the association of phenol, we also determined its T_1^{DD} values in CCl_4 and $CHCl_3$, the latter data being corrected for its different viscosity (Table 2).

NMR measurements on monofunctional acceptors: **Pyridine/phenol as a test case**: According to FT-IR measurements, $x_{HB} = 0.82$ when both concentrations are 0.5 M. The system was firstly investigated by measuring variations in chemical shift and T_1 of the ^{14}N signal for pyridine, varying the total concentration in CCl_4 (from 1.00 to 0.05 M) at a constant 1:1 pyridine:phenol ratio. A small (6 ppm) and erratic chemical shift change, and a regular T_1 increase (from 0.20 to 0.39 ms) with decreasing concentration, are found.

In a 0.5 M solution, the addition of an equivalent amount of phenol slightly shields the signal ($\Delta\delta = -12$), but the most prominent spectral change is a major line broadening, $W_{1/2}$ increasing from 216 to 911 Hz (T_1 decreasing from 1.59 to 0.23 ms) (Figure 1, Table 3). These spectral changes are

0947-6539/00/0616-2918 $ 17.50+.50/0 *Chem. Eur. J.* **2000**, *6*, No. 16

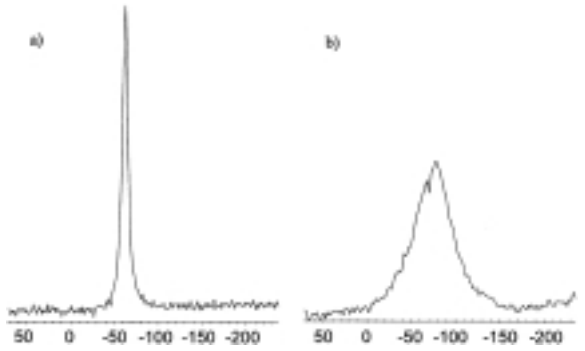

Figure 1. ^{14}N-NMR spectra of 0.5 M pyridine in CCl_4: a) pure, b) after addition of one equivalent of phenol.

actually due to HB formation, since analogous experiments using anisole (not a HB donor[8]) or 2,6-di-*tert*-butylphenol (sterically hindered around the OH group[39]) showed no appreciable variation in chemical shift and width of the ^{14}N signal for pyridine.

The calculated efg change for the PhOH···py complex (Table 1) is $\chi_{eff}^{R} = 0.80$, that is HB is predicted to cause a 20% efg decrease at the pyridine nitrogen. A comparison of experimental T_1 values as such would imply the opposite trend, since $T_1^0/T_1^{HB} = 6.9$. Given the large extent of HB formation, the effect of molecular dynamics clearly prevails over that of the efg in determining T_1, that is the line broadening observed stems from an increase of τ_c (slower molecular motion). This was checked by analyzing ^{13}C-NMR data (Table 3). From the T_1^{DD} for pyridine C-4 and using the calculated r_{CH} (1.076 Å), we calculate $\tau_c^0 = 1.4$ ps and $\tau_c^{HB} =$ 14 ps. Introducing these values in Equation (2), the resulting experimental efg variation is $\chi_{eff}^{R} = 0.69$. Even though this value does not exactly match the calculated value, it shows that calculated and experimental efg changes are comparable.

Introducing ^{13}C T_1^{DD} values for C-2 or C-3 in Equation (2) $\chi_{eff}^{R} > 1$ is obtained, in disagreement with the theoretical prediction. This arises because only the motion of C-4 describes the motion of the entire complex, and hence has the correlation time sought, while C-2 and C-3 describe also rotations around the H-N-C-4 axis. In fact, τ_c(C-4) increases by 10 times, while τ_c(C-2) and τ_c(C-3) increase only by 4–5 times; this indicates that the mobility of the complex is less reduced along those axes. This finding highlights the need to properly select the carbon atom(s) for estimating τ_c changes.

In order to evaluate the solvent effect, measurements were run also in $CHCl_3$ for pyridine with MTA and phenol (assuming x_{HB} as in CCl_4) (Table 3). The contribution from dynamics was again evaluated on C-4. The data for the remaining monofunctional acceptors are also reported in Table 3.

Nitriles and carbonyl acceptors: Nitriles present the serious drawback that the cyano carbon (the best choice for the determination of τ_c) has a very long T_1 and a low NOE value. HB formation resulted in a 3 to 5 ppm shielding of the nitrogen nucleus. Benzonitrile was then chosen as an alternative, owing to the presence of at least one carbon atom (C-4) potentially appropriate for a reliable determination of τ_c. For such measurements we used the x_{HB} value found for acetonitrile.

The same concerns about τ_c determination observed for acetonitrile again apply to the carbonyl carbon of acetone. The ^{17}O nucleus in HB complexes is more shielded (by 3–20 ppm) than in free acceptors. Benzaldehyde (a weaker acceptor than acetone) was then chosen as an alternative

Table 3. ^{14}N-, ^{17}O- and ^{13}C-NMR parameters for monofunctional HB acceptors in hydrogen-bonded systems.[a]

Acceptor/Solvent		Acceptor nucleus			^{13}C					
Donor	x_{HB}		δ	T_1 [ms][b]	ass.	δ	T_1 [s]	η[c]	T_1^{DD} [s]	χ_{eff}^{R} [d]
pyridine/CCl_4[e]		^{14}N	−63	1.59	C-4	135.5	18.6	1.2	30.8	–
phenol[f]	0.82		−75	0.23		137.0	2.6	1.7	3.1	0.69
pyridine/$CHCl_3$		^{14}N	−70	1.05	C-4	135.9	12.8	1.5	17.0	–
phenol	0.82[g]		−82	0.35		137.0	3.9	1.8	4.3	0.75
MTA	0.79		−77	0.54		136.4	6.0	1.7	7.0	0.78
acetonitrile/CCl_4		^{14}N	−130	2.43	*C*N	115.1	34.0	0.15	450	–
phenol	0.79		−135	0.82		116.0	18.4	0.16	229	1.56
benzonitrile/CCl_4		^{14}N	−121	0.59	C-4	132.7	5.4	1.7	6.3	–
phenol	0.79[h]		−123	0.34		133.1	3.3	1.7	3.8	1.13 (1.21)
benzonitrile/$CHCl_3$		^{14}N	−127	0.65	C-4	132.7	7.0	1.9	7.4	–
MTA	0.79		−131	0.58		132.8	5.2	2.2	4.7	0.67 (0.72)
acetone/CCl_4		^{17}O	585	7.0	*C*O	202.7	24.9	0.12	412	–
phenol	0.83		565	3.3		207.8	31.5	0.19	329	1.81
benzaldehyde/CCl_4		^{17}O	574	1.95	*C*O	190.5	16.2	1.5	21.2	–
phenol	0.76		557	1.58		192.6	9.8	1.7	11.7	0.63 (0.64)
benzaldehyde/$CHCl_3$		^{17}O	556	2.13	*C*O	192.3	13.9	1.7	16.6	–
phenol	0.76[g]		548	1.93		193.2	11.3	1.7	12.9	0.80 (0.78)
MTA	0.70		553	1.98		192.7	12.4	1.8	13.4	0.83 (0.87, 0.85)

[a] Both donor and acceptor 0.5 M in the specified solvent, except where indicated. [b] For ^{17}O these are T_2* values obtained from line widths, except where specified. [c] NOE enhancement. [d] See Equation (2). Values in brackets have been recalculated with the correction for the anisotropy of motion (see Equations (3)–(5)). When two values are given, the second one refers to the calculated complex with two donor molecules. [e] Correlation times of C-4-H, C-3-H and C-2-H vectors, calculated assuming $r_{CH} = 1.076$, 1.077, 1.074 Å are 1.4, 1.4, and 1.3 ps, respectively. [f] Correlation times of C-4-H, C-3-H and C-2-H vectors, calculated assuming the same r_{CH} values are 14, 4.5, and 5.0 ps, respectively. [g] Assumed equal to the value in CCl_4. [h] Assumed equal to the value for CH_3CN.

along the lines seen before. We also studied the complex with phenol and MTA in $CHCl_3$, assuming the x_{HB} value found in CCl_4.

Hydrogen bonds of amides: ***N,N*-dimethylformamide and *N,N*-dimethylbenzamide (DBA)**: The study of HB formation on amides is complicated by the presence of both a donor (N–H in primary and secondary amides) and an acceptor group (oxygen), which in fact is at the basis of their importance in biological systems.

N,N-Dimethylformamide (DMF) was chosen for modeling amide HBs since it can only act as acceptor (supposedly via the oxygen[2]) and because the carbonyl carbon bears a hydrogen. Addition of phenol (in CCl_4) causes the usual spectral changes (Table 4). Measurements were also run with MTA in $CHCl_3$, but unfortunately the two ^{17}O signals are not resolved.

N,N-Dimethylbenzamide was selected with the criteria already discussed, and was studied in association with phenol in CCl_4 and $CHCl_3$ (x_{HB} was assumed to be 0.90, that is a slightly lower value than for the corresponding DMF complexes) and with MTA in $CHCl_3$ ($x_{HB} = 0.80$ was assumed). Given the peculiar results from the first system (see Discussion), ^{17}O-enriched DBA was employed in order to directly measure T_1 and hence to rule out the difference between T_2^* and T_1 as a possible source of error. In this case, however, severe signal overlap in the ^{14}N spectra prevented us from obtaining a reliable T_1 value.

Anisotropic diffusion in HB complexes: As we have seen, a critical point in the interpretation of T_1 changes is the contribution of molecular dynamics. For an accurate evaluation of this term, the possible anisotropy of rotational diffusion should be considered. If molecular tumbling is isotropic, the correlation time extracted from T_1^{DD} values does not depend on the carbon atom observed. Otherwise, different correlation times will be measured according to the orientation of the C–H bond used for the determination of T_1^{DD}. In this case, only a carbon atom with a C–H bond parallel to q_{zz} would provide the correct τ_c, but this condition is not always met (e.g., in benzaldehyde). The effect of anisotropic motion can be corrected for in rigid aromatic molecules, as follows. The quadrupolar relaxation rate in anisotropically tumbling molecules is given by Equation (3):[40, 41]

$$\frac{1}{T_1} = K\chi_{eff}(A\cos^2\Psi + B\sin^2\Psi) \quad (3)$$

where Ψ is the angle defined by the direction of q_{zz} and one of the principal axes of rotational diffusion, and $A = [3(D_y+D_z)]^{-1}$, $B = [3(D_x+D_z)]^{-1}$, where D_i are the elements of the diagonalized diffusion tensor.[41] Thus, a highly anisotropic motion is characterized by an A/B ratio very different from unity. Dipole–dipole relaxation data from ^{13}C NMR can be used to obtain values of A and B according to Equation (4) (Figure 2):

$$\frac{1}{T_1^{DD}(j)} = \left(\frac{\mu_0}{4\pi}\right)^2 \hbar^2\gamma_C^2\gamma_H^2 [A\sum_i r_{ij}^{-6}\cos^2\Psi_{ij} + B\sum_i r_{ij}^{-6}\sin^2\Psi_{ij}] \quad (4)$$

where r_{ij} is the distance between the i-th hydrogen and the j-th carbon, and Ψ_{ij} is the angle between the C–H vector and one of the main axes of rotational diffusion.

Let us consider carbon atoms bonded to a single hydrogen. If ϕ_{ij} is the angle between the C–H vector and an arbitrary reference axis forming an angle θ with respect to the principal axis of diffusion,

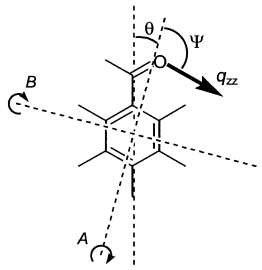

Figure 2. Parameters appearing in Equations (3)–(5) for benzaldehyde.

Table 4. ^{14}N-, ^{17}O- and ^{13}C-NMR parameters for polyfunctional HB acceptors in hydrogen-bonded systems.[a]

Acceptor/Solvent		Acceptor nucleus			^{13}C					
Donor	x_{HB}		δ	T_1 [ms]	ass.	δ	T_1 [s]	η	T_1^{DD} [s]	χ_{eff}^R
***N,N*-dimethylformamide/CCl_4**		^{17}O	335	5.71	*C*O	161.2	22.0	1.2	36.3	
		^{14}N	–281	1.71						
phenol	0.94	^{17}O	311	2.72	*C*O	162.7	9.4	1.7	11.0	0.63
		^{14}N	–275	0.71						0.72
***N,N*-dimethylformamide/$CHCl_3$**		^{17}O	312	5.30	*C*O	162.4	14.9	1.6	19.0	
		^{14}N	–276	1.91						
MTA	0.85	^{17}O	[b]		*C*O	162.6	*12*	1.6	*15*	
		^{14}N	–275	1.58						0.93
phenol	0.94	^{17}O	301	3.68	*C*O	163.0	11.3	1.7	13.4	1.02
		^{14}N	–272	1.32						1.02
***N,N*-dimethylbenzamide/CCl_4**		^{17}O	353	0.72	C-4	129.5	3.1	1.9	3.3	
		^{14}N	–284	0.36						
phenol	0.90	^{17}O	327	0.37	C-4	129.6	2.5	1.6	3.0	1.89 (1.70)
		^{14}N	–287	0.20						1.69 (1.38)
***N,N*-dimethylbenzamide/$CHCl_3$**		^{17}O	334	0.70	C-4	129.7	3.4	1.4	4.8	
		^{14}N	–280	0.43						
MTA	0.80	^{17}O	329	0.47	C-4	129.5	3.0	1.8	3.2	1.00
										(0.96, 0.95)
		^{14}N	[b]							
phenol	0.90	^{17}O	322	0.73	C-4	129.2	3.5	1.6	4.2	0.83 (0.74)
		^{14}N	–278	0.33						1.17 (0.95)

[a] See footnotes [b]–[d] in Table 3. [b] Unresolved spectrum.

0947-6539/00/0616-2920 $ 17.50+.50/0 *Chem. Eur. J.* **2000**, *6*, No. 16

and ϕ_q the angle between q_{zz} and the same arbitrary axis, Equation (4) can be rewritten as Equation (5):

$$\frac{1}{T_1^{DD}(j)}\left(\frac{\mu_0}{4\pi}\right)^2 \hbar^2\gamma_C^2\gamma_H^2 r_{ij}^{-6}[A+(B-A)\sin^2(\phi_{ij}+\theta)] \quad (5)$$

where A, B, and θ are parameters to be optimized by fitting ab initio values obtained for r_{ij}, ϕ_{ij}, and experimental ones for $T_1^{DD}(j)$. Efg changes corrected for anisotropic diffusion (Table 4) have been calculated from Equation (5) with the fitted A, B and, θ values, substituting $\Psi_{ij}=\phi_{ij}+\theta$ and $\Psi=\phi_q+\theta$. The complete data are available as Supporting Information.

Discussion

Calculated geometries and electric field gradients: We will first comment on the relative performance of the basis sets used for geometry optimization, that is 6-31G(d,p) and 6-311G(d,p) at the HF level. For all systems reported in Table 1, optimization with the larger basis brings an increase in HB binding energies (by 0.1–0.3 kcal mol^{-1}), and the geometries (r and α) undergo changes of $\pm$0.01–0.02 Å and $\pm$0.1–0.5°, respectively. However, if the efg values are calculated with the same basis (6-311G(d,p)) no appreciable variation in absolute and, especially, relative efg values is found, since χ_{eff} values change by $\pm$0.2–2.0 MHz[2] (i.e., $<$10%), and χ_{eff}^R values by $\pm$0.01–0.02. Hence, the different level of geometry optimization has no major effect in the calculated efg values, even if the respective geometries are somewhat different. Correlated levels of theory (MP2 or DFT) are known to yield shorter HB distances.[6] However, since MP2 geometry optimizations are notoriously very expensive, we ran some tests with a DFT method which performs very well on HB systems at a much lower cost.[26] The comparison of HF and DFT calculations on two test systems (pyridine/phenol and benzaldehyde/phenol) has, however, shown that, even though the geometry is somewhat different, the efg thus calculated is, again, affected only to a small extent.

Hence, although the relative performance of HF, MPn or DFT methods in the understanding of HB and the calculation of **q** is of interest in itself,[35] for the scope of the present investigation the choice of either basis set for geometry optimization, as well as the theoretical method, is largely irrelevant, since the resulting χ_{eff}^R values are very similar. Hereafter, for consistency we will only discuss results obtained at the HF/6-311G(d,p)//6-311G(d,p) level.

All HBs considered herein involve neutral species, and hence are relatively weak. However, the theoretical level adopted is not sufficient for a reliable modeling of the HB strength; hence, we will only mention that E_b values lie between -3 and -16 kcal mol^{-1}.

Calculated r values lie between 1.5 and 2.1 Å, and α between 150° and 180°, that is in their normal ranges.[2] However, it is worthwhile to mention that the geometry of approach of either donor to carbonyl acceptors is frequently off the carbonyl plane, especially with MTA. Such arrangements are in fact often found in protein inter-residue HBs.[2]

HB formation causes a decrease in the calculated efg at the acceptor nucleus, $\chi_{eff}^R < 1$ being always predicted. Such changes (as well as the corresponding chemical shift changes) qualitatively match those found for analogous proton-transfer equilibria.[32, 35] Thus, both protonation and HB formation at an amino or pyridino nitrogen entail a marked efg decrease; however, in the former case the change is much larger, χ_{eff}^R being 10^{-7}–10^{-2}.[32b, 35]

Other things being equal, the calculated HB distance (r) and χ_{eff} variation (χ_{eff}^R) increase in the series $CF_3OH < PhOH < CF_3CONHCH_3$, that is theoretical predictions are remarkably dependent on the donor molecule. Hereafter, we will only compare experimental and theoretical results obtained with the same donor.

Generally, NMR measurements also report $\chi_{eff}^R < 1$, but the decrease of χ_{eff} is larger than calculated. The effect of various experimental factors is discussed below.

Effects of solvent, donor, and anisotropy of motion on experimental efg changes: As we have seen, changes in the molecular dynamics (τ_c) constitute a major source of T_1 change, which in fact agrees with the relatively small efg changes calculated for HB formation. Even after correcting for this, experimental T_1s were found to depend on other factors, as follows.

The decrease of χ_{eff} experimentally observed upon addition of phenol is smaller in $CHCl_3$ than in CCl_4. This behavior likely arises from the weak but non-negligible HB donor properties of $CHCl_3$.[8] In fact, calculations for the $H_2C{=}O\cdots(HCCl_3)_2$ complex yield $\chi_{eff}^R = 0.86$ even though r is 2.3 Å, while the same calculations with CCl_4 (where r is much longer) yield $\chi_{eff}^R = 1.00$, as expected for a non-interacting molecule. Thus, if the solvent $CHCl_3$ hydrogen bonds to the acceptor, the assumption of having a free acceptor breaks down, and its χ_{eff} in the "free" state is lower than assumed. According to this hypothesis, the measured χ_{eff}^R would be the ratio between the complex with phenol and a complex with $CHCl_3$. For example, the decrease of efg for benzaldehyde from CCl_4 to $CHCl_3$ is $\chi_{eff}^R = 0.71$, which is definitely not negligible. If this is the case, obviously the experimental system becomes very difficult to compare with the calculated one, since even a 2:1 complex can hardly be expected to model a system in which the donor is the solvent itself.

A further complication regarding phenol concerns the probable formation of hydrogen-bonded dimers or oligomers of the type PhOH$\cdots$O(H)Ph. The extent of this aggregation is also solvent-dependent, as highlighted by the analysis of ^{13}C relaxation data of phenol (Table 2). On going from CCl_4 to $CHCl_3$, these relaxation times become longer to a different extent for each ring carbon (3% for C-3, 52% for C-4), which probably indicates that phenol oligomers dissociate in $CHCl_3$. If the phenol dimer acts as donor, the strength of the donor OH is enhanced by the HB between the two phenol molecules.[42] Calculations for the $(PhOH)_2\cdots$py complex show a decrease of χ_{eff}^R from 0.80 to 0.75 with respect to PhOH$\cdots$py. Therefore, if the actual donor is the dimer (or a related oligomer), smaller χ_{eff}^R values than those predicted for 1:1 complexes should be expected.

Hence, phenol is an inherently complicated system, since in CCl_4 it is largely aggregated, while in $CHCl_3$ it is less so but the solvent is not inert. Although aggregation cannot occur for MTA, the same concerns regarding $CHCl_3$ as solvent still apply; in neither case the system lends itself to a simple modeling.

The correction for the anisotropy of motion generally leads to a better agreement between experimental and theoretical data, provided that the uncorrected values also follow the correct trend. In fact, if the experimental $\chi^R_{eff} > 1$ the assumptions for an evaluation of the complex structure (and for the correction itself) fail. Interesting information about the anisotropy of diffusion can be derived from the ratio A/B, which gives a quantitative indication of the motional anisotropy.

Pyridine: Experimentally (in CCl_4) $\chi^R_{eff} = 0.69$, the calculated value being 0.80. The values become closer if the comparison is made with the complex with the phenol dimer ($\chi^R_{eff} = 0.75$). In $CHCl_3$ $\chi^R_{eff} = 0.75$, in excellent agreement with the complex calculated for the phenol dimer. The measurements with MTA provide a better agreement between experimental ($\chi^R_{eff} = 0.78$) and calculated (0.81) values. For free pyridine, rotational diffusion is isotropic ($A/B = 1.0$), while in the phenol complex it becomes highly anisotropic ($A/B = 9.5$). However, correcting for the anisotropy of motion does not bring any appreciable change to the results, which indicates that the C-4 pyridine carbon provides by itself a reliable indication of the dynamics changes occurring upon complex formation.

Nitriles: The χ^R_{eff} value for CH_3CN with PhOH in CCl_4 (1.56) is at variance with theoretical predictions (0.84 – 0.86). In this case, the discrepancy stems from the inadequacy of NMR data, since the relevance of T_1^{DD} data for the cyano carbon is uncertain, due to the very low NOE. For benzonitrile too, HB with phenol causes an efg increase ($\chi^R_{eff} = 1.13$) rather than the expected decrease (0.84). For the MTA complexes the change (0.67) is instead in fair agreement with the calculated value of 0.85. Correcting for the anisotropy of motion does not improve the phenol results, since they lack an acceptable starting point. For the MTA complex, the corrected χ^R_{eff} (0.72) is closer to the ab initio prediction.

Carbonyl acceptors: Calculated χ_{eff} values for 2:1 complexes are always smaller than for 1:1 complexes, implying a higher symmetry at the oxygen in the former. Use of these models reduces the difference between experimental and theoretical data, as detailed below. Therefore, it seems that carbonyl acceptors indeed form HBs of this type to a large extent.

For PhOH/acetone, experimental results are once more against theoretical predictions for the reasons seen for acetonitrile. In order to circumvent these problems, benzaldehyde was studied. The experimental χ^R_{eff} in CCl_4 (0.63) is smaller than the calculated one (0.89), but is, at least, < 1. For the ternary complex $\chi^R_{eff} = 0.77$, with a smaller discrepancy. The solvent effect is analogous to that on pyridine; hence, on switching to $CHCl_3$ χ^R_{eff} becomes larger (0.80) and closer to the theoretical value for the ternary complex. χ^R_{eff} is even smaller for the MTA complex (0.83). The theoretical value (0.86) is only slightly different, and the discrepancy becomes even smaller after correcting for the anisotropy of motion (0.87). Considering the ternary complex we again have an excellent agreement, the calculated χ^R_{eff} being 0.79 versus a corrected experimental value of 0.85. This correction does not bring appreciable changes in the case of phenol complexes; hence, also in this case the dynamics of motion probed by the C-4 carbon of the acceptor seem reliable.

Amides: *a) DMF*: Calculated χ^R_{eff} values for the O- and N-bound complex with phenol are not very different (O-bound: 0.70 for ^{17}O and 0.86 for ^{14}N; N-bound: 0.80 for ^{17}O and 0.88 for ^{14}N). The calculated values for the 2PhOH$\cdots$DMF O-bound complex (0.63 for ^{17}O and 0.76 for ^{14}N) are lower. Experimental χ^R_{eff} values in CCl_4 (0.63 for ^{17}O and 0.72 for ^{14}N) are, in fact, in excellent agreement with the latter. On the other hand, χ^R_{eff} values in $CHCl_3$ are very close to unity (1.02 for ^{17}O and ^{14}N).

b) N,N-Dimethylbenzamide: In CCl_4, χ^R_{eff} values are > 1 (1.89 for ^{17}O and 1.69 for ^{14}N), and hence in disagreement with the calculated values (0.88 for both ^{17}O and ^{14}N in the O-bound complex). Rotational diffusion is anisotropic for the free acceptor ($A/B = 2.3 - 2.6$), but becomes almost isotropic for the complex with phenol ($A/B = 1.1$). This correction leads to a marked decrease of χ^R_{eff}, which, however, remain > 1. In $CHCl_3$, χ_{eff} variations are smaller, as usual (0.83 for ^{17}O and 1.17 for ^{14}N), and the value for oxygen becomes < 1. Correcting for anisotropy, χ^R_{eff} values become < 1 for both nuclei (0.74 for ^{17}O and 0.95 for ^{14}N). Diffusion remains anisotropic for the complex with MTA ($A/B = 2.0$) but becomes again almost isotropic with phenol ($A/B = 1.2$). For the complex with MTA, the agreement between experimental (corrected for anisotropy: 0.96 for ^{17}O) and theoretical data (0.92) is good; the results for the ternary complex are similar.

In all cases efg changes do not differentiate well between *N*- and *O*-HB. This is not an important issue in itself, since *O*-HB in amides is well established, but suggests that the easier to observe ^{14}N nucleus can be just as useful as ^{17}O in probing amide HB. However, one can expect difficulties due to the rather small efg changes, especially for the 2:1 complexes which seem to be a decidedly better model.

Conclusion

The formation of a hydrogen bond causes readily measurable changes in the parameters of the NMR relaxation of the quadrupolar acceptor nucleus. Therefore, a variation of efg can reveal not only the formation, but also some structural characteristics of the hydrogen bond, since it depends on the change in the symmetry of the surroundings, and hence on the position of the bridged hydrogen. Normally a decrease in the relaxation time is observed, but this is entirely due to an increase in the correlation time, which can be conveniently highlighted through ^{13}C relaxation. When this correction can be done in a dependable way (i.e., when suitable ^{13}C nuclei are available) the change in electric field gradient (χ^R_{eff}) can be extracted from the observed T_1 change.

Experimental and calculated χ^R_{eff} values are compared in Figure 3. For most acceptors there is a very good agreement, as can be appreciated by the comparison with the unit-slope line. This is even more remarkable if one considers the small

  0947-6539/00/0616-2922 $ 17.50+.50/0 *Chem. Eur. J.* **2000**, *6*, No. 16

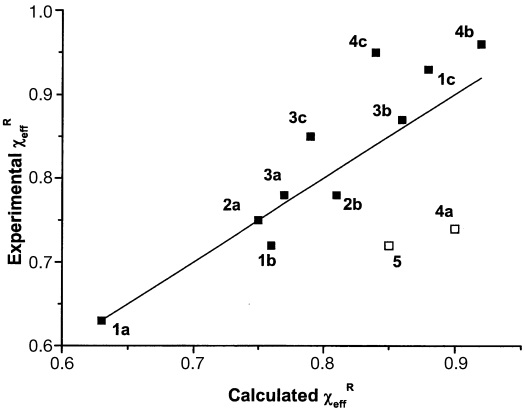

Figure 3. Comparison of calculated and experimental χ_{eff}^{R} values; the line has unit slope. Data for the acceptor nucleus, except where indicated. Theoretical model and experimental conditions are given for each acceptor (denoted by the boldface number). **1**, DMF (via O): a) 2:1 complex with phenol, solvent CCl_4, data for ^{17}O; b) same data for ^{14}N; c) 1:1 complex with MTA, solvent $CHCl_3$. **2**, pyridine: a) 1:1 complex with $(PhOH)_2$, solvent $CHCl_3$; b) 1:1 complex with MTA, solvent $CHCl_3$. **3**, benzaldehyde: a) 2:1 complex with phenol, solvent $CHCl_3$, correction for anisotropy; b) 1:1 complex with MTA, solvent $CHCl_3$, correction for anisotropy; c) 2:1 complex with MTA, solvent $CHCl_3$, correction for anisotropy. **4**, *N*,*N*-dimethylbenzamide (via O): a) 2:1 complex with phenol, solvent CCl_4, correction for anisotropy; b) 1:1 complex with MTA, solvent $CHCl_3$, correction for anisotropy; c) 2:1 complex with MTA, solvent $CHCl_3$, correction for anisotropy. **5**, benzonitrile: 1:1 complex with MTA, solvent $CHCl_3$, correction for anisotropy.

range spanned by the values (0.6–1.0). For two acceptors (benzonitrile and *N*,*N*-dimethylbenzamide) the agreement is much less satisfactory. At present, we can only account for these discrepancies as due to averaging over other HB structures (e.g., higher complexes than 1:1 or 2:1, or with different geometries of approach) that may be present in solution but are not correctly modeled, which further highlights the need of properly selecting a theoretical model. Thus, the combined theoretical/experimental approach adopted seems generally adequate to model efg changes occurring upon HB formation, as long as one keeps in mind the large structural variability and the complex dynamics of these HB complexes.

We finally remark that any future application of this method to large molecules shall cope with very broad line widths due to their slow motion. However, as pointed out by Germann et al.,[43] at currently available high magnetic field strengths ($\geq$17.6 T) certain nuclear transitions of half-integer quadrupolar nuclei give rise to relatively narrow signals, which opens the way to an extension of the concepts presented herein to such systems.

Experimental Section

Reagents and solvents: Commercial phenol, CCl_4, $CHCl_3$, CH_3CN, pyridine, acetone, DMF, and methyl trifluoroacetate were purified by standard methods. ^{17}O-enriched water (Yeda, $^{17}O = 10.4\,\%$, $^{18}O = 56.8\,\%$) and remaining compounds were used as received. *N*-Methyltrifluoroacetamide (MTA) was prepared by aminolysis of methyl trifluoroacetate with methylamine.[44]

Synthesis of ^{17}O-enriched *N*,*N*-dimethylbenzamide: a) ^{17}O-Enriched benzoyl chloride:[45] To a well-stirred mixture of $PhCCl_3$ (8 mL, 56.5 mmol) and $FeCl_3 \cdot 6H_2O$ (0.02 g, 74 μmol) heated at 110 °C and protected by a reflux condenser, ^{17}O-enriched water (0.8 mL, 43.5 mmol) was added dropwise by means of a syringe within 90 min. Distillation at reduced pressure yielded $PhC^{17}OCl$ (5.04 g, 79 %). B.p. 70 °C; GC-MS: *m*/*z* (%): 144 (1), 142 (4), 141 (1), 140 $[^{16}O - M]^+$ (2), 108 (6), 107 (82), 106 (19), 105 (51). By comparison with a natural abundance sample [*m*/*z* (%): 142 (1), 140 $[M]^+$ (4), 106 (7), 105 (100)], an ^{17}O content of 11 atom % was estimated.

b) A mixture of of $PhC^{17}OCl$ (4.84 g, 34.4 mmol) and DMF (6.09 g, 83.3 mmol) was heated under reflux under stirring at 155 °C for 3 h. The product was distilled at reduced pressure (b.p. 80–94 °C) and yielded $PhC^{17}ONMe_2$ (0.33 g, 79 %).[46] GC-MS: *m*/*z* (%): 151 (4), 150 (13), 149 $[^{16}O - M]^+$ (20), 148 (50), 119 (1), 108 (1), 107 (21), 106 (12), 105 (100). By comparison with a natural abundance sample [*m*/*z* (%): 150 (2), 149 $[M]^+$ (16), 148 (46), 119 (1), 106 (8), 105 (100)], an ^{17}O content of 3 atom % was estimated.

NMR and IR measurements: ^{13}C-NMR experiments were carried out on a Bruker AC 250 (5.9 T, 250.1 MHz for ^1H, 62.9 MHz for ^{13}C). ^{14}N and ^{17}O experiments were performed on a Bruker AM 400 or Avance DRX 400 (9.4 T; 400.13 MHz for ^1H, 28.91 MHz for ^{14}N, 54.24 MHz for ^{17}O). Some ^{14}N-NMR experiments were carried out on a Bruker Avance DMX 600 (14.1 T, 43.35 MHz for ^{14}N). All spectra were recorded at 298 K in 10 mm tubes for ^{14}N and ^{17}O (natural abundance) spectra or 5 mm tubes for ^{17}O-(labelled samples) and ^{13}C-NMR spectra. Measurements in chloroform were performed with $CHCl_3$ (^{14}N, ^{17}O) or $CDCl_3$ (^{13}C). Samples for ^{13}C were degassed with three freeze–pump–thaw cycles. ^{14}N and ^{17}O T_1s were determined by inversion-recovery, with acoustic ringing suppression[47] where necessary, and ^{13}C T_1s by saturation-recovery. ^{14}N- and ^{17}O-NMR chemical shifts are externally referenced to neat CH_3NO_2 and H_2O, respectively. Kinematic viscosities were determined using an Ubbelohde viscometer at 25 ± 0.01 °C.

FT-IR measurements were performed on a Perkin–Elmer 1600 instrument with a 1 mm BaF_2 cell (resolution 4 cm^{-1}, 256 scans). We monitored the phenol O–H stretching peak (ca. 3610 cm^{-1} for the free donor, and lower wavenumbers for the complex).[10, 11] For MTA we observed the free N–H stretching peak at 3460 cm^{-1} for (vs. 3300 cm^{-1} for the complex). The complex mole fraction (x_{HB}) was determined directly from measurements on a solution at the concentration and ratio of interest.

Experimental procedure: The relaxation times T_1 for the acceptor nuclei (^{14}N and ^{17}O), as well as the T_1 and NOE of a suitable ^{13}C nucleus in the acceptor, are determined before and after adding an equivalent amount of donor. The incomplete formation of HB is accounted for as follows. Under fast-exchange conditions, the observed relaxation rate in the presence of the donor is given by a weighted averages like $R_1 = R_1^0 x_0 + R_1^{HB} x_{HB}$, or $R_1 \propto \chi_{eff}^0 \tau_c^0 x_0 + \chi_{eff}^{HB} \tau_c^{HB} x_{HB}$. The observed dipolar relaxation rate is likewise given by $R_1^{DD} = R_1^{DD,0} x_0 + R_1^{DD,HB} x_{HB}$. Substituting these equations into $\chi_{eff}^{HB}/\chi_{eff}^0 = (T_1^0/T_1^{HB})(\tau_c^0/\tau_c^{HB})$, Equation (2) is obtained. If x_{HB} is independently known, for example from FT-IR measurements, Equation (2) can be evaluated to yield χ_{eff}^{R}.

[1] S. Scheiner, *Molecular Interactions*, Wiley, London, **1997**.
[2] G. A. Jeffrey, W. Saenger, *Hydrogen Bonding in Biological Structures*, Springer, Berlin, **1991**.
[3] F. Hibbert, J. Emsley, *Adv. Phys. Org. Chem.* **1990**, *26*, 255.
[4] J. C. MacDonald, G. M. Whitesides, *Chem. Rev.* **1994**, *94*, 2383.
[5] J. Bernstein, M. C. Etter, L. Leiserowitz, in *Structure Correlation* (Eds.: H.-B. Bürgi, J. D. Dunitz), VCH, Weinheim, **1994**.
[6] U. Koch, P. L. A. Popelier, *J. Phys. Chem.* **1995**, *99*, 9747.
[7] For recent leading references see: a) B. Schwartz, D. G. Drueckhammer, *J. Am. Chem. Soc.* **1995**, *117*, 11902; b) C. L. Perrin, Y.-J. Kim, *J. Am. Chem. Soc.* **1998**, *120*, 12641; c) Y. Kato, L. M. Toledo, J. Rebek, *J. Am. Chem. Soc.* **1996**, *118*, 8575; d) M. Garcia-Villoca, R. Gelabert, A. Gonzalez-Lafont, M. Moreno, J. M. Lluch, *J. Am. Chem. Soc.* **1998**, *120*, 10203; e) Y. Pan, M. A. McAllister, *J. Am. Chem. Soc.* **1998**, *120*, 166; f) N. S. Golubev, I. G. Shenderovich, S. N. Smirnov, G. S. Denisov, H. H. Limbach, *Chem. Eur. J.* **1999**, *5*, 492.
[8] M. H. Abraham, *Chem. Soc. Rev.* **1993**, *22*, 73.
[9] R. W. Taft, D. Gurka, L. Joris, P. von R. Schleyer, J. W. Rakshys, *J. Am. Chem. Soc.* **1969**, *91*, 4801.
[10] D. Gurka, R. W. Taft, *J. Am. Chem. Soc.* **1969**, *91*, 4794.

[11] M. Berthelot, F. Besseau, C. Laurence, *Eur. J. Org. Chem.* **1998**, 925, and previous papers by the same group.
[12] J. Marco, J. M. Orza, R. Notario, J. L. M. Abboud, *J. Am. Chem. Soc.* **1994**, *116*, 8841.
[13] a) E. M. Arnett, L. Joris, E. Mitchell, T. S. S. R. Murty, T. M. Gorrie, P. von R. Schleyer, *J. Am. Chem. Soc.* **1970**, *92*, 2365; b) R. Gurka, R. W. Taft, *J. Am. Chem. Soc.* **1969**, *91*, 4794; c) R. W. Taft, D. Gurka, L. Joris, P. von R. Schleyer, J. W. Rakshys, *J. Am. Chem. Soc.* **1969**, *91*, 4801; d) L. Joris, J. Mitsky, R. W. Taft, *J. Am. Chem. Soc.* **1972**, *94*, 3438.
[14] a) A. Bagno, G. Scorrano, S. Stiz, *J. Am. Chem. Soc.* **1997**, *119*, 2299; b) A. Bagno, M. Campulla, M. Pirana, G. Scorrano, S. Stiz, *Chem. Eur. J.* **1999**, *5*, 1160.
[15] G. Wider, R. Riek, K. Wüthrich, *J. Am. Chem. Soc.* **1996**, *118*, 11629.
[16] G. Q. Wagner, *Rev. Biophys.* **1983**, *16*, 1.
[17] L. J. Altman, D. Laungani, G. Gunnarsson, H. Wennerström, S. Forsén, *J. Am. Chem. Soc.* **1978**, *100*, 8264.
[18] a) N. Juranic, P. K. Ilich, S. Macura, *J. Am. Chem. Soc.* **1995**, *117*, 405; b) F. Cordier, S. Grzesiek, *J. Am. Chem. Soc.* **1999**, *121*, 1601.
[19] a) A. J. Dingley, S. Grzesiek, *J. Am. Chem. Soc.* **1998**, *120*, 8293; b) K. Pervushin, A. Ono, C. Fernandez, T. Szyperski, M. Kainosho, K. Wüthrich, *Proc. Natl. Acad. Sci. USA* **1998**, *95*, 14147.
[20] G. Cornilescu, J.-S. Hu, A. Bax, *J. Am. Chem. Soc.* **1999**, *121*, 2949.
[21] a) N. Tjandra, A. Bax, *J. Am. Chem. Soc.* **1997**, *119*, 8076; b) M. Tessari, H. Vis, R. Boelens, R. Kaptein, G. W. Vuister, *J. Am. Chem. Soc.* **1997**, *119*, 8985.
[22] a) J. Boyd, T. K. Mal, N. Soffe, I. D. Campbell, *J. Magn. Reson.* **1997**, *124*, 61; b) A. C. LiWang, A. Bax, *J. Magn. Reson.* **1997**, *127*, 54.
[23] S. N. Smirnov, N. S. Golubev, G. S Denisov, H. Benedict, P. Schah-Mohammedi, H. H. Limbach, *J. Am. Chem. Soc.* **1996**, *118*, 4094.
[24] H. Benedict, H. H. Limbach, M. Wehlan, W. P. Fehlhammer, N. S. Golubev, R. Janoschek, *J. Am. Chem. Soc.* **1998**, *120*, 2939.
[25] a) J. D. Dill, L. C. Allen, W. C. Topp, J. A. Pople, *J. Am. Chem. Soc.* **1975**, *97*, 7220; b) P. Hobza, J. Sauer, *Theor. Chim. Acta* **1984**, *65*, 279; c) M. J. Frisch, J. A. Pople, J. E. Del Bene, *J. Phys. Chem.* **1985**, *89*, 3664; d) J. J. Novoa, M. H. Whangbo, *J. Am. Chem. Soc.* **1991**, *113*, 9017; e) Y. C. Tse, M. D. Newton, L. C. Allen, *Chem. Phys. Lett.* **1980**, *75*, 350.
[26] For some recent references see: a) J. E. Del Bene, W. B. Person, K. Szczepaniak, *J. Phys. Chem.* **1995**, *99*, 10705; b) M. W. Feiereisen, D. Feller, D. A. Dixon, *J. Phys. Chem.* **1996**, *100*, 2993; c) I. N. Demetropoulos, I. P. Gerothanassis, C. Vakka, C. Kakavas, *J. Chem. Soc. Faraday Trans.* **1996**, *92*, 921; d) W. G. Han, S. Suhai, *J. Phys. Chem.* **1996**, *100*, 3942; e) M. Lozynski, D. Rusinska-Roszak, H. G. Mack, *J. Phys. Chem. B* **1998**, *102*, 2899; f) P. R. Rablen, J. W. Lockman, W. L. Jorgensen, *J. Phys. Chem. A* **1998**, *102*, 3782; g) H. Guo, D. R. Salahub, *Angew. Chem.* **1998**, *110*, 3155; *Angew. Chem. Int. Ed.* **1998**, *37*, 2985.
[27] C. A. Deakyne, M. Mautner, *J. Am. Chem. Soc.* **1999**, *121*, 1546, and previous papers by the same group.
[28] a) G. Desiraju, *Acc. Chem. Res.* **1996**, *29*, 441; b) I. Alkorta, I. Rozas, J. Elguero, *Chem. Soc. Rev.* **1998**, *27*, 163; c) P. Hobza, V. Spirko, Z. Havlas, K. Buchhold, B. Reimann, H.-D. Barth, B. Brutschy, *Chem. Phys. Lett.* **1999**, *299*, 180.
[29] M. Ramos, I. Alkorta, J. Elguero, N. S. Golubev, G. S. Denisov, H. Benedict, H. H. Limbach, *J. Phys. Chem. A* **1997**, *101*, 9791.
[30] *Multinuclear NMR* (Ed.: J. Mason), Plenum Press, London, **1987**.
[31] IUPAC recommends the symbol η for the asymmetry parameter (R. K. Harris, J. Kowalewski, S. Cabral de Menezes, *Magn. Reson. Chem.* **1998**, *36*, 145). To avoid confusion with the symbol for the NOE we use here the other common symbol ε.
[32] a) A. Bagno, C. Comuzzi, G. Scorrano, *J. Am. Chem. Soc.* **1994**, *116*, 916; b) A. Bagno, B. Bujnicki, S. Bertrand, C. Comuzzi, F. Dorigo, P. Janvier, G. Scorrano, *Chem. Eur. J.* **1999**, *5*, 523, and references cited therein.
[33] A. D. Becke, *J. Chem. Phys.* **1993**, *98*, 5648.
[34] L. G. Butler, in *^{17}O NMR Spectroscopy in Organic Chemistry* (Ed.: D. W. Boykin), CRC Press, Boca Raton, **1991**.
[35] A. Bagno, G. Scorrano, *J. Phys. Chem.* **1996**, *100*, 1545, and references cited therein.
[36] M. J. Frisch, G. W. Trucks, H. B. Schlegel, G. E. Scuseria, M. A. Robb, J. R. Cheeseman, V. G. Zakrzewski, J. A. Montgomery, Jr., R. E. Stratmann, J. C. Burant, S. Dapprich, J. M. Millam, A. D. Daniels, K. N. Kudin, M. C. Strain, O. Farkas, J. Tomasi, V. Barone, M. Cossi, R. Cammi, B. Mennucci, C. Pomelli, C. Adamo, S. Clifford, J. Ochterski, G. A. Petersson, P. Y. Ayala, Q. Cui, K. Morokuma, D. K. Malick, A. D. Rabuck, K. Raghavachari, J. B. Foresman, J. Cioslowski, J. V. Ortiz, B. B. Stefanov, G. Liu, A. Liashenko, P. Piskorz, I. Komaromi, R. Gomperts, R. L. Martin, D. J. Fox, T. Keith, M. A. Al-Laham, C. Y. Peng, A. Nanayakkara, C. Gonzalez, M. Challacombe, P. M. W. Gill, B. Johnson, W. Chen, M. W. Wong, J. L. Andres, C. Gonzalez, M. Head-Gordon, E. S. Replogle, J. A. Pople, *Gaussian 98*, *Revision A.6*, Gaussian, Inc., Pittsburgh PA, **1998**.
[37] K. B. Wiberg, M. Marquez, H. Castejon, *J. Org. Chem.* **1994**, *59*, 6817.
[38] P. Murray-Rust, J. P. Glusker, *J. Am. Chem. Soc.* **1984**, *106*, 1018.
[39] A. Bagno, R. L. Boso, N. Ferrari, G. Scorrano, *Eur. J. Org. Chem.* **1999**, 1507.
[40] a) W. T. Huntress, *Adv. Magn. Reson.* **1970**, *4*, 1; b) W. T. Huntress, *J. Chem. Phys.* **1968**, *48*, 3524.
[41] L. M. Jackman, J. C. Trewella, R. C. Haddon, *J. Am. Chem. Soc.* **1980**, *102*, 2519.
[42] F. Ramondo, L. Bencivenni, G. Portalone, A. Domenicano, *Struct. Chem.* **1995**, *6*, 37.
[43] W. Germann, J. M. Aramini, H. J. Vogel, *J. Am. Chem. Soc.* **1994**, *116*, 6971.
[44] E. R. Bissel, M. Finger, *J. Am. Chem. Soc.* **1954**, *76*, 1372.
[45] W. von E. Doering, K. Okamoto, K. Krauch, *J. Am. Chem. Soc.* **1960**, *82*, 3579.
[46] G. M. Coppinger, *J. Am. Chem. Soc.* **1954**, *76*, 1372.
[47] A. Bagno, *Magn. Reson. Chem.* **1992**, *30*, 1164.
[48] *CRC Handbook of Chemistry and Physics* (Ed.: D. R. Lide), 77th ed., CRC Press, Boca Raton, **1997**.

Received: July 19, 1999
Revised version: March 20, 2000 [F1928]

  0947-6539/00/0616-2924 $ 17.50+.50/0